particles

MDPI

Review

Electromagnetic Field and Radiation of Charged Particles in the Vicinity of Schwarzschild Black Hole

Stanislav Komarov [1,2,*] and Gregory Vereshchagin [2,3,4,5]

1 Department of Theoretical Physics and Astrophysics, Belarusian State University, 4 Nezavisimosti Ave., 220030 Minsk, Belarus
2 ICRANet-Minsk, National Academy of Sciences of Belarus, 68-2 Nezavisimosti Ave., 220072 Minsk, Belarus; veresh@icra.it
3 ICRANet, Piazza della Repubblica, 10, 65122 Pescara, Italy
4 INAF—IAPS, Via del Fosso del Cavaliere, 100, 00133 Rome, Italy
5 ICRA, Dipartimento di Fisica, Sapienza Università di Roma, Piazzale Aldo Moro 5, 00185 Rome, Italy
* Correspondence: staskomarov@tut.by

Abstract: We provide a concise review of the problem of calculating the electromagnetic field and radiation of a charged particle in the vicinity of a black hole. The interest in this problem has been revived due to recent progress in multimessenger observations. Many astrophysical models of energy extraction from a black hole involve consideration of such motion and radiation. Our main goal is to highlight the basic assumptions and limitations of various techniques and point out the main conclusions of these studies.

Keywords: black holes; electromagnetic radiation; Regge–Wheeler equation

check for updates

Academic Editors: Maxim Yu. Khlopov and Armen Sedrakian

Received: 16 October 2024
Revised: 3 December 2024
Accepted: 17 December 2024
Published: 30 December 2024

Citation: Komarov, S.; Vereshchagin, G. Electromagnetic Field and Radiation of Charged Particles in the Vicinity of Schwarzschild Black Hole. *Particles* **2025**, *8*, 1. https://doi.org/10.3390/particles8010001

1. Introduction

The dynamics of electromagnetic fields and electromagnetic radiation of charged particles moving in the vicinity of a black hole are relevant in many astrophysical problems, and they are involved in the description of active galactic nuclei, X-ray binaries, and microquasars. Recently, the interest in this subject has been revived due to the realization that magnetized black holes may accelerate particles [1–3] and, thus, produce strong electromagnetic signals [4,5], charging black holes [6]. This is an important subject for models of energy extraction from black holes, e.g., [7–12].

Given the fact that the problem under consideration is quite involved [13], the solution is approached in steps. The first step is the determination of the electromagnetic field of a static charge outside the black hole. Then, the dynamical problem is addressed with the motion of a charge without radiation. Next, the problem of a charge (mass) emitting electromagnetic (gravitational) radiation is considered. Finally, the radiation reaction on the motion of the charge is taken into account.

The simplest case of a charged particle in a gravitational field is a test charge fixed in a given geometry. The electric field of such fixed electric charge in the field of a Schwarzschild black hole is considered in [14–16]. The electric and magnetic fields of a charged ring around a black hole are considered in [17–19].

However, particles cannot stay at rest near black holes without external support; hence, consideration of moving charges is necessary. Accelerated charges emit electromagnetic radiation. The simplest case, emission by a charge, radially falling into a Schwarzschild black hole was considered in [20], adopting the expression for emitted power for flat spacetime.

Particle motion and radiation have been considered for a spherically symmetric black hole, e.g., in [21–24]; for a rotating black hole, e.g., in [25–28]; and, more recently, with a focus on magnetized black holes, e.g., in [29–33]. The general approach to the evaluation of electromagnetic fields of a particle moving near a Schwarzschild black hole was developed in [34] by expanding Maxwell equations in multipoles. The spectra of the first few multipoles together with the total radiated energy were found in [35,36]. Recently, more multipoles were computed in [37]. The studies of electromagnetic fields and radiation of a charged particle are closely related to the studies of gravitational radiation of a massive particle in a gravitational field. Indeed, perturbation techniques developed in the 1970s [38–40] allowed the consideration of not only perturbations of the gravitational field of black holes and their stability but also the interaction of scalar, vector, and tensor fields in curved spacetime around black holes.

Finally, by approximating the potential barrier in the Regge–Wheeler equation with the Dirac delta function and rectangular barrier, it was shown [41] that the electromagnetic field of a charge falling into a Schwarzschild black hole exponentially approaches the spherically symmetric electrostatic field.

The scope of this paper is to review the basic results and illustrate novel approaches to the problem of radiation of charged particles near a Schwarzschild black hole. The paper is organized as follows. First, we review different approaches to the problem in Section 2. Then, we discuss a general formalism in Section 3. Equations of motion are given in Section 4. Multipolar decomposition of the electromagnetic field of a charged particle moving near a black hole is given in Section 5. Radiated power and energy are discussed in Section 6. The cases of radial motion and non-radial motion are described in Sections 7 and 8, correspondingly. Stationary component of the electromagnetic field is discussed in Section 9. Finally, we conclude in Section 10.

2. State of the Art

Different approaches to the study of electromagnetic fields of charged particles around black holes can be summarized as follows.

2.1. Electrostatic Electromagnetic Field of a Charge Near Schwarzschild Black Hole

The first attempts to compute the electromagnetic energy of a charge in curved background geometry were based on the assumption that the charge is at rest. The electrostatic field of a test charge in the Schwarzschild metric was found by Copson [14] in 1928. Physical properties of this solution were analyzed by Hanni and Ruffini [16], with particular attention to the lines of force of a charge located near the event horizon. The complete derivation of the exact analytic solution was finally given by Linet [15]. What is interesting in the solution of Linet is that when the charge is located precisely on the event horizon of a black hole, its electromagnetic field becomes spherically symmetric. In other words, the charge appears to be uniformly distributed over the horizon. Clearly, this solution is different from the Reisnner–Nordström solution, as there is no charge *inside* the horizon. However, the exterior solution in this case is indistinguishable from the Reisnner–Nordström solution.

2.2. Special Relativistic Calculation for Radiation Power for a Particle Following Geodesic on a Given Background

The cases of radial infall and finite motion of the charged particle in the vicinity of the Schwarzschild black hole were considered in [20]. The power of electromagnetic radiation is calculated using the formula for flat spacetime:

$$dP^{\hat{i}} = \frac{2q^2}{3}\frac{d^2x^{\hat{k}}}{d\tau^2}\frac{d^2x_{\hat{k}}}{d\tau^2}u^{\hat{i}}d\tau\,. \qquad (1)$$

where $x^{\hat{k}}$ is the Cartesian coordinates of the particle, $u^{\hat{i}}$ is its four-velocity, q is electric charge, and τ is the proper time of the particle.

As the charge moving near the horizon gets accelerated to relativistic velocities, its emission gets concentrated in a narrow angle in the direction of motion. For radial infall, this implies that most of the radiation is captured by the black hole.

Also, gravitational radiation of this particle is considered. It is shown that the whole electromagnetic energy radiated by an electron falling into a black hole is 10^{43} times larger than the gravitational energy radiated by this electron.

Electromagnetic radiation of pointlike charged test particles and dipoles is considered also in [42]. It is shown that the electromagnetic radiation for the point particle, as well as for the electric dipole, has a dipolar character (the emitted energy is $\sim 1/c^2$). It is also pointed out that the whole energy of electromagnetic radiation for the case of a black hole with mass $< 10^{14}$ g is larger than its rest energy mc^2, which implies that a quantum description of such black holes is required.

2.3. General Relativistic Calculation of Electromagnetic Field for Test Particle Falling Radially into a Black Hole

A more interesting problem concerns the description of electromagnetic radiation as well as the motion of the particle in the framework of General Relativity, considered in [34–36]. In these works, it is shown that the Fourier transform of the multipole components of the electromagnetic field satisfies the well-known Regge–Wheeler equation [35,38,39,43]. The numerical solution of this equation for a number of multipoles gives a possibility to determine the physical characteristics of electromagnetic radiation, such as total radiated energy and its spectrum.

The fully general-relativistic treatment of the electromagnetic radiation of a particle falling into the Reisnner–Nordström black hole is presented in [34]. It is important to stress that the radiation reaction is nevertheless neglected. The main results of these studies can be summarized as follows:

- The largest part of the radiated electromagnetic energy (about 90%) corresponds to the dipole term;
- In particular, for initial kinetic energy (E) per unit mass (m) of the particle $E/m = 1.4$, the total radiated energy was found to be $\approx 10^{-2} q^2/M$, where q is particle charge, M is black hole mass;
- For the case of a charged particle (with negative charge) falling into a charged black hole (with positive charge), the contribution to the radiated energy of higher multipoles ($l > 1$) is more significant than in the case of an electrically neutral black hole.

2.4. A Complex Angular Momentum Description

Electromagnetic radiation of the charged particle falling into a black hole radially and moving along circular orbits has been calculated recently using the alternative description based on the evaluation of Regge poles of the S-matrix, associated with complex amplitudes of the solutions of the Regge–Wheeler equation. The mathematical technique, which also applies to the calculation of gravitational waves and other black hole perturbations [44,45] is based on analytic continuation of both frequency and angular momentum into the complex plane, see [46] for earlier work. The application of this formalism to electromagnetic radiation of a charged particle plunging from below the last circular orbit was performed in [47], while the calculation of electromagnetic emission for a radially falling particle was conducted in [37]. Also, radiated energy as a function of time was calculated for both cases using the Sommerfeld–Watson approach. This method allows the calculation of intensity of radiation and radiated spectrum for a large number of multipoles.

2.5. Non-Radial Motion and Calculation of Non-Gravitational Radiation Reaction Force

In [48], the case of charged particle motion in the vicinity of a magnetized Schwarzschild black hole is considered. It was shown that Formula (1) can be applied only when the curvature of particle trajectory is much smaller than the spacetime curvature. The direction of particle motion was assumed to be such that the deviation of the trajectory from the magnetic field is opposite to the deviation from the gravitational field. In that case, the condition of applicability of Equation (1) is satisfied. The main conclusion is that initial non-geodesic orbital motion, which has loops due to the magnetic field, decays as a consequence of the synchrotron radiation, and the final trajectory is a non-geodesic stable circular orbit.

The influence of the radiation reaction force on the motion of the charged particle in the vicinity of the Schwarzschild black hole is taken into account in [49]. The formulas for calculating the influence of spacetime curvature on electromagnetic radiation are presented, but all results are obtained neglecting the curvature. The motion and electromagnetic radiation of the particle in the field of a magnetized black hole are also considered. The following results are obtained:

- The whole electromagnetic energy, radiated by the charged particle, falling into a black hole from rest at infinity is $\approx 0.022q^2/M$.
- The radiated energy calculated using general relativistic treatment exceeds the radiated energy by a factor of few, calculated using Formula (1).
- For black holes with mass $M \sim M_\odot$, where $M_\odot$ is the mass of the Sun, the characteristic frequency of electromagnetic radiation is $10^4 Hz$.
- In contrast with the radiation emitted outward from the black hole, the power of electromagnetic radiation emitted towards the black hole is not decreasing with multipole number l.

3. A General Formalism for the Calculation of Electromagnetic Fields Created by Moving Particles in Curved Spacetime

Consider a charged test particle, moving in the gravitational field of a Schwarzschild black hole. Electromagnetic radiation of the particle can be found from the general covariant Maxwell equations (see, e.g., [50]):

$$F^{ls}{}_{;s} = 4\pi j^l \,, \tag{2}$$

$$F_{[ij,k]} = 0 \,. \tag{3}$$

Here, J^l is the electric current density, created by the particle, and F^{ij} is the tensor of electromagnetic field. It follows from Equation (3) that tensor F_{ij} can be expressed as

$$F_{ij} = A_{j;i} - A_{i;j} \,; \tag{4}$$

where A_i is the four-potential of the electromagnetic field. In the case of a pointlike charged particle, j^l can be represented as

$$j^l(x^k) = q \frac{\delta(x^1 - \tilde{x}^1(x^0))\delta(x^2 - \tilde{x}^2(x^0))\delta(x^3 - \tilde{x}^3(x^0))}{\sqrt{-g}u^4(x^0, \tilde{x}^\alpha(x^0))} \times u^l(x^0, \tilde{x}^\alpha(x^0)) \,. \tag{5}$$

Here, $g = \det(g_{ij})$. Coordinates with a tilde $\tilde{x}^i$ are functions describing the worldline of the source and without tilde x^i are arbitrary coordinates of spacetime.

The modern approach to the derivation of electromagnetic radiation and equations of motion of charged particles taking into account radiation reaction in curved spacetime is presented by Poisson [51]. According to the results of this paper, the general solution of

(2) and (3) with source (5) for the four-potential of electromagnetic field A^j can be expressed using Synge's world function σ, which is a two-point scalar (biscalar) [52]. Define the geodesic curve as a curve in spacetime with local minimum length between two fixed points (events) $\mathcal{X}_1$ and $\mathcal{X}_2$: $\int_{\mathcal{X}_1}^{\mathcal{X}_2} \mathrm{d}s = \int_{\mathcal{X}_1}^{\mathcal{X}_2} \sqrt{|g_{ij}\mathrm{d}x^i\mathrm{d}x^j|}$ = extremum (see also [53]). For the general parametrization of the curve $x^i = x^i(\nu)$, this leads to the differential equation

$$\frac{\mathrm{d}^2x^i}{\mathrm{d}\nu^2} + \frac{\mathrm{d}x^i}{\mathrm{d}\nu}A(\nu) + \Gamma^i_{jk}\frac{\mathrm{d}x^j}{\mathrm{d}\nu}\frac{\mathrm{d}x^k}{\mathrm{d}\nu} = 0\,. \tag{6}$$

Here, $A(\nu)$ is the certain function that is determined by $x^i(\nu)$ [50]. In order to simplify (6), one can solve the following differential equation:

$$A(\nu) = \left(\frac{\mathrm{d}\lambda}{\mathrm{d}\nu}\right)^2 \frac{\mathrm{d}^2\nu}{\mathrm{d}\lambda^2}\,. \tag{7}$$

A solution of (7) λ is called the affine parameter along the geodesic $x^i(\lambda)$. In the obtained parametrization, the geodesic equation has a simpler form:

$$\frac{Dx^k}{D\lambda} = \frac{\mathrm{d}^2x^i}{\mathrm{d}\lambda^2} + \Gamma^i_{jk}\frac{\mathrm{d}x^j}{\mathrm{d}\lambda}\frac{\mathrm{d}x^k}{\mathrm{d}\lambda} = 0\,.$$

It is well known that massive particles in the absence of non-gravitational interaction move along timelike geodesics (see, e.g., [50,53]). Proper time of the particle τ can be used as affine parameter in this case and $u^i = \frac{\mathrm{d}x^i}{\mathrm{d}\tau}$, $u^iu_i = -c^2$. Isotropic geodesics are characterized by another property of the tangent vector $k^i = \frac{\mathrm{d}x^i}{\mathrm{d}\lambda}$, namely, $k^ik_i = 0$. Only massless particles, such as photons, move along isotropic geodesics. Proper time for photons cannot be determined; thus, affine parameter λ for the isotropic geodesics has no simple physical interpretation.

Synge's World function $\sigma(x,\, x')$ can be expressed as

$$\sigma(x,\, x') = \frac{1}{2}(\lambda_1 - \lambda_0)\int_{\lambda_0}^{\lambda_1} g_{ij}t^it^j\mathrm{d}\lambda\,, \tag{8}$$

where $\lambda \in [\lambda_0,\, \lambda_1]$ is an affine parameter on geodesic, connecting initial point x (that corresponds to the value λ_0) and final point x' (that corresponds to the value λ_1, see Figure 1).

Here, we define unit tangent vector to the geodesic in arbitrary point z: $t^j = dz^j/d\lambda$ ($||t||^2 = g_{ij}t^it^j = \pm 1$, where the sign depends on whether the geodesic is timelike or spacelike. In the case of isotropic geodesic, the norm is 0.). Also, we use the following abbreviation for covariant derivatives of biscalar σ (D/Dx^i denotes covariant derivative at the point x, while $D/Dx^{i'}$ denotes covariant derivative at the point x'):

$$\frac{\partial}{\partial x^l}\sigma(x,\, x') = \sigma_l\,; \quad \frac{\partial}{\partial x^{l'}}\sigma(x,\, x') = \sigma_{l'}\,;$$
$$g^{ms}\frac{D}{Dx^m}\frac{\partial}{\partial x^{l'}}\sigma(x,\, x') = \sigma^s{}_{l'}\,; \ldots$$

The general solution for electromagnetic potential A_l has the following form:

$$A^l = q\frac{u^{l'}g^l{}_{l'}\sqrt{\Delta}}{\sigma_{k'}u^{k'}}\bigg|_{\sigma=0} + q\int_{-\infty}^{\tau'} V^l{}_{l''}u^{l''}\mathrm{d}\tau''\,. \tag{9}$$

Here, q is the charge of the particle, $\Delta = -\det\left[g^{l}{}_{l'}\sigma^{l'}{}_{m}\right]$ is the van Vleck determinant. $V_{ii'}$ is a bitensor satisfying d'Alembert's equation in the curved spacetime

$$g^{ij}\frac{D^2}{Dx^i Dx^j}V^{l}{}_{l''} - R^{l}{}_{s}V^{s}{}_{l''} = 0\,, \tag{10}$$

and the initial condition is in the following form:

$$V_{l'l'} = \frac{1}{12}Rg_{l'l'} - \frac{1}{2}R_{l'l'}\,; \tag{11}$$

Condition $\sigma = 0$ in (9) means that the corresponding expression must be calculated at the point x', connected with argument point x by an isotropic geodesic.

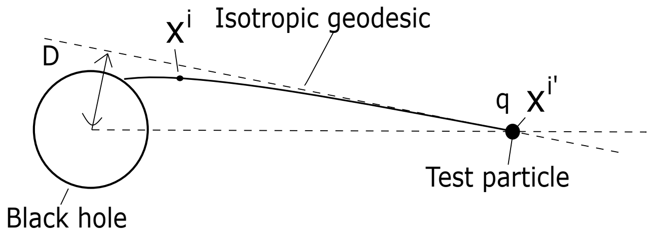

Figure 1. An isotropic geodesic connecting the particle in $x^{i'}$ and the point of observation x^i.

The obtained four potential (9) is used in order to obtain the equation of motion of the test charge in curved spacetime that undergoes an electromagnetic radiation reaction force [51]:

$$m\frac{\mathrm{D}u_i}{\mathrm{D}\tau} = qF^{ext}_{ij}u^j - \frac{2q^2}{3s}\frac{\mathrm{D}u_i}{\mathrm{D}\tau} + q\left(g_{ij} + u_i u_j\right)\left(\frac{2}{3}\frac{D^2u^j}{D\tau^2} + \frac{1}{3}R^{j}{}_{k}u^k\right) + F^{\mathrm{tail}}_i\,. \tag{12}$$

Here, F^{ext}_{ij} is the external electromagnetic field, and we have introduced the tail term $F^{\mathrm{tail}}_i = \int\limits_{-\infty}^{\tau} V_{ii';j}u^{i'}u^j \mathrm{d}\tau'$. In the absence of external electromagnetic field ($F^{ext}_{ij} = 0$), if we neglect the tail term F^{tail}_i in equation (12), the geodesic motion satisfies this equation and moving charge does not experience radiation reaction. It is obvious that the radiation reaction in purely gravitational field (without electromagnetic one) is determined by the tail term. This conclusion was obtained in [54], where numerical estimations of the influence of the tail term on the motion of the charge were made.

In general, calculation of the F^{tail}_i is a very complicated task (see, e.g., [55,56]). The approximation of small velocity of motion and small distance was calculated by De Witt and De Witt [55] using the analogy with the quantum field theory. The same result was obtained in [56] in the framework of post-Newtonian expansion in General Relativity. The result is

$$F^{\mathrm{tail}}_{\alpha} = \frac{q^2 M x^{\alpha}}{r^4} - \frac{2q^2 M}{3}\left(\frac{v^{\alpha}}{r^3} - 3\frac{x^{\alpha}(x_{\beta}v^{\beta})}{r^5}\right). \tag{13}$$

Here, v^{α} is the usual 3-dimension velocity of the test-charge, $r = \sqrt{x_{\alpha}x^{\alpha}}$.

In the special case when the charge is at rest in the vicinity of Schwarzschild black hole, the tail term was calculated in [57]. In this paper, consideration based on the calculation of Synge's World function for a large distance from a black hole was applied and electromagnetic self-force was computed. The radial component of the self-force F_r was found to be

$$F_r \approx q^2\int\limits_{-\infty}^{0} V_{ji'';r}u^{i''}g^{j}{}_{k''}u^{k''}\mathrm{d}\tau'' \approx \frac{q^2 M}{r'^3}. \tag{14}$$

This result coincides with the results, obtained in the framework of membrane paradigm (see, e.g., [58]), and with those obtained from different approaches (see, e.g., [59,60]) and Formula (13) (for $v^\alpha = 0$).

The self-force in the form (14) for the test charge at rest in the field of Schwarzschild black hole is also obtained in [61], where the stress–energy tensor conservation law was used. The physical consequences of this force for the black holes with different masses are also discussed there.

In what follows, we concentrate on the most widely used approach based on multipolar expansion of electromagnetic fields. Before that, we review the basic results of geodesic motion in Schwarzschild geometry.

4. Geodesic Motion in Schwarzschild Geometry

Assume that electromagnetic radiation of the particle cannot influence its motion, which implies that radiation reaction is neglected. So, in what follows, we consider only the geodesic motion of the particle, which is determined by the equation

$$\frac{Du^i}{D\tau} = 0\,. \tag{15}$$

Here, $D/D\tau$ denotes the covariant derivative with respect to proper time τ along vector u^i. The exact conditions under which radiation reaction force can be neglected are discussed, for instance, in [49].

Consider a test particle that moves along a geodesic in Schwarzschild geometry. Let x^i (We use the system of units where the speed of light in vacuum is $c = 1$. The signature of the metric is +2, $x^0 = t$. Greek indices run from 1 to 3; Latin indices run from 0 to 4) be coordinates of the particle, τ its proper time, and $u^i = \mathrm{d}x^i/\mathrm{d}\tau$ its four-velocity. Metric in the case of Schwarzschild geometry has the following form (see, e.g., [50]):

$$\mathrm{d}s^2 = g_{ij}\mathrm{d}x^i\mathrm{d}x^j = -\left(1 - \frac{2M}{r}\right)\mathrm{d}t^2 + \frac{\mathrm{d}r^2}{\left(1 - \frac{2M}{r}\right)} + r^2\mathrm{d}\theta^2 + r^2\sin^2\theta\,\mathrm{d}\phi^2\,. \tag{16}$$

Here, g_{ij} is the metric tensor; $\{t, r, \theta, \phi\} = \{x^0, x^1, x^2, x^3\}$ are Schwarzschild coordinates; and $M = Gm_{BH}$, where m_{BH} is the black hole mass and G is Newton's gravitational constant.

Solving the geodesic Equation (15) for the metric (16), we obtain the following result (see, e.g., [50]):

$$\begin{cases} u^0 = \dfrac{E}{\left(1 - \frac{2M}{r}\right)}\,; \\ u^1 = \pm\sqrt{E^2 - \left(1 + \dfrac{L^2}{r^2}\right)\left(1 - \dfrac{2M}{r}\right)}\,; \\ u^2 = 0\,; \\ u^3 = \dfrac{L}{r^2}\,. \end{cases} \tag{17}$$

Here, we choose the orientation of the spatial part of the coordinate system in such a way that the orbit plane coincides with the plane $\theta = \pi/2$. E is the energy of the particle per unit mass, and L is the angular momentum of the particle per unit mass. The sign $\pm$ in the formula for u^1 corresponds to the motion from the field center and to the field center, respectively.

It is well known that the equation for u^1 (see (17)) can be used to introduce the effective potential $V(r)$ [50] (see also Figure 2):

$$\left(\frac{\mathrm{d}r}{\mathrm{d}\tau}\right)^2 = E^2 - V(r)\,. \tag{18}$$

Here,

$$V(r) = \left(1 + \frac{L^2}{r^2}\right)\left(1 - \frac{2M}{r}\right). \tag{19}$$

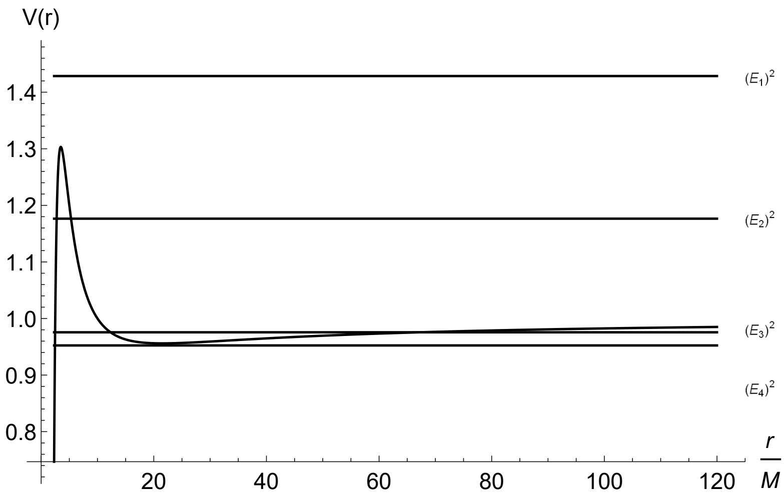

Figure 2. Effective potential $V(r)$ for radial motion in Schwarzschild geometry for $L = 5M$. E_1, E_2, E_3, E_4 denote four qualitatively different levels of the energy per unit mass of the test particle.

Effective potential for $L = 5M$ and four levels of the energy per unit mass for the test particle are depicted in Figure 2. The values of the energy per unit mass E_1 correspond to the trajectories when the particle is falling into the black hole. The value E_2 corresponds to the case when the particle comes from the spatial infinity goes through the pericenter of the orbit and moves to the spatial infinity. The value E_3 corresponds to the finite motion of the particle in the vicinity of the black hole. The value E_4 is a special case of the finite motion when the trajectory of the particle is a circle.

Using equations for the components of the four-velocity vector (17), we can construct the differential equation for the trajectory of the test particle (see, e.g., [50]). An example of the trajectory of motion corresponding to the type of trajectory with energy $E2$ (see Figure 2) is presented in Figure 3.

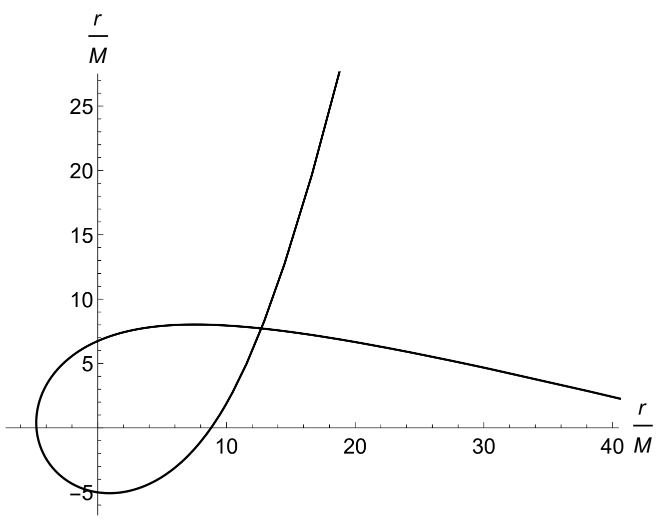

Figure 3. Example of the trajectory of a test particle in Schwarzschild geometry. Energy per unit mass of the particle $E = 1.05$ and angular momentum per unit mass $L = 4.5M$.

5. Electromagnetic Field of a Charged Test Particle in Schwarzschild Geometry

The solution of Equations (2)–(4) for the radiated electromagnetic field can be found in the following form (see, e.g., [36,62]):

$$\begin{cases} A_0 = \sum\limits_{m=-l}^{l} \sum\limits_{l=0}^{\infty} f_{lm}(r,t) Y_{lm}(\theta,\phi)\,, \\ A_1 = \sum\limits_{m=-l}^{l} \sum\limits_{l=0}^{\infty} h_{lm}(r,t) Y_{lm}(\theta,\phi)\,, \\ A_2 = \sum\limits_{m=-l}^{l} \sum\limits_{l=0}^{\infty} k_{lm}(r,t) \dfrac{\partial Y_{lm}(\theta,\phi)}{\partial\theta} + \dfrac{a_{lm}(r,t)}{\sin\theta} \dfrac{\partial Y_{lm}(\theta,\phi)}{\partial\phi}\,, \\ A_3 = \sum\limits_{m=-l}^{l} \sum\limits_{l=0}^{\infty} k_{lm}(r,t) \dfrac{\partial Y_{lm}(\theta,\phi)}{\partial\phi} - \dfrac{a_{lm}(r,t)}{\sin\theta} \dfrac{\partial Y_{lm}(\theta,\phi)}{\partial\theta}\,. \end{cases} \tag{20}$$

Here, $Y_{lm}(\theta,\phi)$ are spherical functions [63]. $f_{lm}(r,t)$, $h_{lm}(r,t)$, $k_{lm}(r,t)$, and $a_{lm}(r,t)$ are certain functions that must be determined. It is convenient to use the following abbreviation:

$$b_{lm} = r^2(h_{lm,t} - f_{lm,r}) \frac{1}{l(l+1)}\,, \text{ if } l > 0\,;$$
$$b_{00} = r^2(h_{00,t} - f_{00,r})\,.$$

We will use the Fourier transform of these functions and denote it by tilde. For example,

$$\begin{cases} \tilde{b}_{lm}(r,\omega) = \dfrac{1}{2\pi} \displaystyle\int_{-\infty}^{+\infty} b_{lm}(r,t) e^{i\omega t} \mathrm{d}t\,; \\ \tilde{a}_{lm}(r,\omega) = \dfrac{1}{2\pi} \displaystyle\int_{-\infty}^{+\infty} a_{lm}(r,t) e^{i\omega t} \mathrm{d}t\,. \end{cases} \tag{21}$$

Substituting (20) into (2) and (4), and using (21), for $\tilde{a}_{lm}(r,t)$, we obtain the following equation:

$$\begin{aligned} &\sum_{m=-l}^{l} \sum_{l=0}^{\infty} \left\{ \left(1 - \frac{2M}{r}\right) \frac{\partial}{\partial r} \left[\left(1 - \frac{2M}{r}\right) \frac{\partial \tilde{a}_{lm}}{\partial r} \right] \right. \\ &\left. + \left[\omega^2 - \frac{l(l+1)}{r^2} \left(1 - \frac{2M}{r}\right) \right] \tilde{a}_{lm} \right\} \\ &\times \left\{ \frac{\partial Y_{lm}}{\partial\theta} + im Y_{lm} \right\} = \sum_{m=-l}^{l} \sum_{l=0}^{\infty} \left[(im-1) \frac{\xi_{lm} Y_{lm}}{\sin\theta} \right]. \end{aligned} \tag{22}$$

In order to obtain equations for coefficients $\tilde{b}_{lm}$, expand components of the current density j^k into spherical functions (the orbit of the particle lies in the plane and, therefore, we can choose the orientation of the coordinate system in such a way that $j_2 = 0$).

$$\begin{cases} 4\pi j_0 = \sum\limits_{m=-l}^{l} \sum\limits_{l=0}^{\infty} \psi_{lm}(r,t) Y_{lm}(\theta,\phi)\,; \\ 4\pi j_1 = \sum\limits_{m=-l}^{l} \sum\limits_{l=0}^{\infty} \eta_{lm}(r,t) Y_{lm}(\theta,\phi)\,; \\ j_2 = 0\,; \\ 4\pi j_3 = \sum\limits_{m=-l}^{l} \sum\limits_{l=0}^{\infty} \xi_{lm}(r,t) Y_{lm}(\theta,\phi)\,. \end{cases} \tag{23}$$

From (2), the following equations are obtained:

$$\eta_{lm}r^2 = -l(l+1)h_{lm} + l(l+1)\frac{\partial k_{lm}}{\partial r} - \frac{l(l+1)}{1-2M/r}\frac{\partial b_{lm}}{\partial t}\,, \tag{24}$$

$$\psi_{lm}r^2 = -l(l+1)f_{lm} + l(l+1)\frac{\partial k_{lm}}{\partial t} - \left(1-\frac{2M}{r}\right)\frac{\partial b_{lm}}{\partial r}l(l+1)\,. \tag{25}$$

Combining Equations (24) and (25), we obtain

$$\left(1-\frac{2M}{r}\right)\left[\left(1-\frac{2M}{r}\right)\tilde{b}_{lm,r}\right]_{,r} + \left[\omega^2 - \frac{l(l+1)}{r^2}\left(1-\frac{2M}{r}\right)\right]\tilde{b}_{lm} = A_{lm}(r)\,. \tag{26}$$

Here,

$$A_{lm}(r) = \left[\left(r^2\tilde{\psi}_{lm}\right)_{,r} + i\omega\tilde{\eta}_{lm}r^2\right]\frac{1}{l(l+1)}\,,\ \text{if } l>0\,; \tag{27}$$

$$A_{00}(r) = \left[\left(r^2\tilde{\psi}_{00}\right)_{,r} + i\omega\tilde{\eta}_{00}r^2\right],\ \text{if } l=0\,. \tag{28}$$

It is convenient to introduce the tortoise coordinate r^*, which can be defined in the region outside the black hole (see, e.g., [50]) as

$$r^*(r) = r + 2M\ln(r/2M-1)\,; \quad \frac{\mathrm{d}r}{\mathrm{d}r^*} = 1-2M/r\,. \tag{29}$$

It follows from the definition that when r changes from $2M$ to ∞ (this corresponds to the region outside the black hole), r^* changes from $-\infty$ to ∞.

Equation (26) is the well-known Regge–Wheeler equation. Boundary conditions for this equation in our case should represent the outgoing wave at spatial infinity and the ingoing wave at the horizon [35,36,64]

$$\tilde{b}_l(r^*,\omega) \to \alpha(\omega)e^{i\omega r^*}\,,\ \text{for } r^* \to +\infty\,; \tag{30a}$$

$$\tilde{b}_l(r^*,\omega) \to \beta(\omega)e^{-i\omega r^*}\,,\ \text{for } r^* \to -\infty\,. \tag{30b}$$

Here, $\alpha(\omega)$ and $\beta(\omega)$ are certain unknown functions.

6. Radiated Power and Energy

The radiated electromagnetic power $\mathrm{d}E/\mathrm{d}t$ can be calculated as an integral of the energy–momentum density T^{0j} through a closed two-dimensional surface, covering the considered system:

$$\frac{\mathrm{d}E}{\mathrm{d}t} = \oint T^{0j}\mathrm{d}\Sigma_j\,. \tag{31}$$

Here, $\mathrm{d}\Sigma_j$ is the element of the surface

$$\mathrm{d}\Sigma_j = \varepsilon_{0jlm}\mathrm{d}_1x^l\mathrm{d}_2x^m\,, \tag{32}$$

where d_1x^l and d_2x^m are infinitesimal linearly independent vectors in . We chose σ as a sphere of radius r with the center that coincides with the position of the black hole. Then, we obtain

$$\frac{\mathrm{d}E}{\mathrm{d}t} = \oint T^{01}r^2\sin\theta\mathrm{d}\theta\mathrm{d}\phi\,. \tag{33}$$

The energy–momentum tensor of electromagnetic field has the following form:

$$T^{ij} = F^{si}F_s{}^j - \frac{1}{4}g^{ij}F^{sl}F_{sl}\,. \tag{34}$$

Substituting (20) into (34) and into (33), we obtain the expression for the power of electromagnetic radiation. This expression is complicated; due to this, here, we write down only the terms that correspond to $m = 0$. The physical meaning of this restriction will be seen in the following sections, where concrete examples of the trajectories of the test particle will be considered. We arrive to

$$\frac{\mathrm{d}E}{\mathrm{d}t} = 2\sum_{l=0}^{\infty}\frac{l(l+1)}{2l+1}\left[\left(\frac{\partial k_{l0}}{\partial t} - f_{l0}\right)\left(\frac{\partial k_{l0}}{\partial r} - h_{l0}\right) + \frac{\partial a_{l0}}{\partial t}\frac{\partial a_{l0}}{\partial r}\right] + M(r,t)\,. \tag{35}$$

Here, $M(r,t)$ denotes part of the expression that is non-zero only if harmonics $m \neq 0$ are present. Further, we can use (25) and (24) in order to simplify expression (35).

The spectrum of radiation $\mathrm{d}E/\mathrm{d}\omega$ is

$$E = \int_{-\infty}^{+\infty}\frac{\mathrm{d}E}{\mathrm{d}t}\mathrm{d}t = 2\sum_{l=0}^{\infty}\frac{l(l+1)}{2l+1} \times \int_{-\infty}^{+\infty}\left[\left(\left(1-\frac{2M}{r}\right)\frac{\partial\tilde{b}_{l0}(\omega,r)}{\partial r} + \frac{\tilde{\psi}_{l0}(\omega,r)r^2}{l(l+1)}\right)\left(\frac{i\omega\tilde{b}_{l0}(-\omega,r)}{1-2M/r} + \frac{\tilde{\eta}_{l0}(-\omega,r)}{l(l+1)}\right) - i\omega\tilde{a}_{l0}(\omega,r)\frac{\partial\tilde{a}_{l0}(-\omega,r)}{\partial r}\right]\mathrm{d}\omega + \int_{-\infty}^{+\infty}M(r,t)\mathrm{d}t\,. \tag{36}$$

7. Radial Motion

Radial motion is the simplest case of the motion in Schwarzschild geometry. It is realized when $L = 0$. The angular component is $u^3 = 0$, and the trajectory of the particle coincides with the coordinate line r. Then, we can choose the orientation of the coordinate system in such a way that the trajectory corresponds to $\theta = 0$. We obtain, see (23),

$$\xi_{lm} = 0\,. \tag{37}$$

Due to the axial symmetry of the problem, the electromagnetic field does not depend on the azimuthal angle ϕ. Consequently, using the representation of spherical functions through associated Legendre polynomials $P_l^m(\cos\theta)$ (see, e.g., [63]),

$$Y_{lm}(\theta,\phi) = P_l^m(\cos\theta)e^{im\phi}\,, \tag{38}$$

we obtain that only components with $m = 0$ can be present in the solution (20). Note that $P_l^0(\cos\theta) = P_l(\cos\theta)$, where $P_l(\cos\theta)$ are usual Legendre polynomials (see, e.g., [63]).

In our case, due to (37) from (22) we obtain a homogeneous differential equation relative to $\tilde{a}_{lm}$. Boundary conditions imply that the electromagnetic field and its derivatives must be null at infinity. Therefore, the unique solution of this equation is $\tilde{a}_{lm} = 0$.

Consequently, in the case of the radial motion of the test particle, the solution for electromagnetic potential can be found in the form

$$\begin{cases} A_0 = \sum\limits_{l=0}^{\infty} f_l(r,t)P_l(\cos\theta)\,, \\ A_1 = \sum\limits_{l=0}^{\infty} h_l(r,t)P_l(\cos\theta)\,, \\ A_2 = \sum\limits_{l=0}^{\infty} k_l(r,t)\dfrac{\mathrm{d}P_l(\cos\theta)}{\mathrm{d}\theta}\,,\ A_3 = 0\,. \end{cases} \tag{39}$$

From (23) and (5), we obtain the following representation for the functions ψ_{lm} and η_{lm} for the case of radial motion ($\xi_{lm} = 0, \theta = 0, \phi = 0, x^1(t) = R(t)$):

$$\psi_{lm}(r,t) = -q\frac{2l+1}{r^2}\left(1 - \frac{2M}{r}\right)\delta(r - R(t))\,; \tag{40}$$

$$\eta_{lm}(r,t) = q\frac{2l+1}{r^2}\left(1 - \frac{2M}{r}\right)\frac{\mathrm{d}R(t)}{\mathrm{d}t}\delta(r - R(t))\,. \tag{41}$$

Here, $r = R(t)$ represents the worldline of the particle.

By using (29); carrying out a Fourier transform of (40), (41); and substituting it into (26), we obtain the following equation:

$$\tilde{b}''_{l0} + \left[\omega^2 - U(r^*)\right]\tilde{b}_{l0} = e^{i\omega T(r)}B_l(r^*)\,, \tag{42}$$

where

$$U(r^*) = \left(1 - \tfrac{2M}{r(r^*)}\right)\tfrac{l(l+1)}{r(r^*)^2}\,, \tag{43}$$

$$B_l(r^*) = \tfrac{q}{2\pi}\tfrac{2l+1}{l(l+1)}\left[T''(r^*) + i\omega(T'(r^*))^2 - i\omega\right], \tag{44}$$

$$B_0(r^*) = \tfrac{q}{2\pi}\left[T''(r^*) + i\omega(T'(r^*))^2 - i\omega\right]. \tag{45}$$

Here, the prime denotes derivative with respect to tortoise coordinate r^* and $T(r^*) = t$ represents the equation of the worldline of the particle. For instance, when the particle starts at the spatial infinity at rest, it has the form

$$T(r^*) = -\tfrac{2}{3\sqrt{2M}}r(r^*)^{3/2} - 2\sqrt{2Mr(r^*)} \\ -2M\ln\left(\tfrac{\sqrt{r(r^*)}-\sqrt{2M}}{\sqrt{r(r^*)}+\sqrt{2M}}\right). \tag{46}$$

For the spectrum of electromagnetic radiation in the case of radial motion from (36), we obtain

$$\frac{\mathrm{d}E}{\mathrm{d}\omega} = 2\sum_{l=0}^{\infty}\frac{l(l+1)}{2l+1}\left(\left(1 - \frac{2M}{r}\right)\frac{\partial\tilde{b}_{l0}(\omega,r)}{\partial r} + \frac{\tilde{\psi}_{l0}(\omega,r)r^2}{l(l+1)}\right) \\ \times\left(\frac{i\omega\tilde{b}_{l0}(-\omega,r)}{1 - 2M/r} + \frac{\tilde{\eta}_{l0}(-\omega,r)}{l(l+1)}\right). \tag{47}$$

Note that, in some papers in the literature, there is a typo in the formula for the spectrum because it does not consist of the term with $\tilde{\psi}_{l0}$, $\tilde{\eta}_{l0}$ (see, e.g., [36]).

From Formula (47), it follows that in order to calculate the spectrum of radiation, it is necessary to solve Equation (42). It is the second kind of non-homogeneous differential equation in which the solution can be obtained using Green's function method (see, e.g., [63]). For this purpose, consider a homogeneous equation, corresponding to (42), for the function $y(r^*)$:

$$y''(r^*) + \left[\omega^2 - U(r^*)\right]y(r^*) = 0\,. \tag{48}$$

Equation (48) has two linearly independent solutions, $y_1(r^*)$ and $y_2(r^*)$. Choose these solutions in such a way that the first solution $y_1(r^*)$ satisfies the boundary condition (30a) and the second solution $y_2(r^*)$ satisfies the boundary condition (30b). These solutions can be expressed through Heun's functions (see, e.g., [43]). Then, the solution of the boundary value problem (30) for $\tilde{b}_{l0}$ has the following form:

$$\tilde{b}_l(r^*,\,\omega) = \frac{1}{W(r^*)}\left[y_1(r^*)\int\limits_{r^*}^{+\infty} y_2(x)a(x)e^{i\omega T(x)}\mathrm{d}x \right.$$
$$\left. + y_2(r^*)\int\limits_{-\infty}^{r^*} y_1(x)a(x)e^{i\omega T(x)}\mathrm{d}x\right], \tag{49}$$

where $W(r^*)$ is the Wronskian of the solutions $y_1(r^*)$ and $y_2(r^*)$:

$$W(r^*) = y_1(r^*)y_2'(r^*) - y_2(r^*)y_1'(r^*)\,. \tag{50}$$

Further simplification of (49) is possible by expressing the functions $y_A(r^*)$ through their derivatives using (48) and performing integration by parts. The result reads

$$\tilde{b}_l(r^*,\omega) = \frac{q}{2\pi}\frac{2l+1}{l(l+1)}\frac{e^{i\omega T(r^*)}}{i\omega} + I\,, \text{ for } l \geq 1\,; \tag{51a}$$

$$\tilde{b}_0(r^*,\omega) = \frac{q}{2\pi}\frac{e^{i\omega T(r^*)}}{i\omega}\,. \tag{51b}$$

Here,

$$I = \frac{y_2(r^*)}{W}\frac{q}{2\pi}\frac{2l+1}{i\omega}\int\limits_{-\infty}^{r^*} U(x)y_1(x)e^{i\omega T}\mathrm{d}x\,. \tag{52}$$

Evaluating integral (52) numerically and substituting it into (51a) and (47), one can obtain the spectrum of radiation. An example of the spectrum of radiation for the different energies of the particle was calculated in [36]. The case of ultrarelativistic initial motion is considered in [65]. The spectrum calculated in [41] is presented in Figure 4.

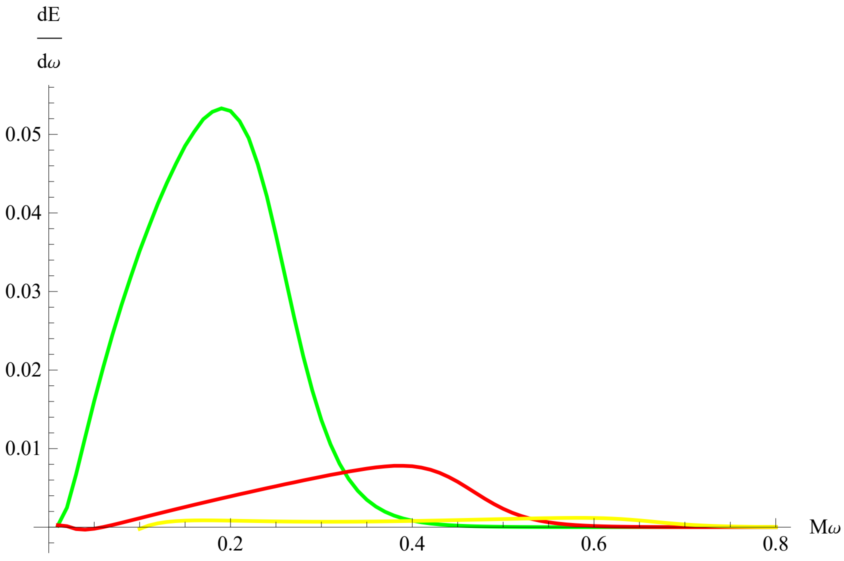

Figure 4. Spectrum of electromagnetic radiation of the particle, falling radially into the Schwarzschild black hole ($q = 1$, $E = 1$), for different multipole indexes $l = 1$ (green), 2 (red), 3 (yellow). The frequency is calculated in units of $1/M$.

8. Non-Radial Motion

In the present section, we consider the case of geodesic non-radial motion of the charged particle in the Schwarzschild geometry. Non-radial motion corresponds to the level of the mechanical energy of the particle, which intersects the effective potential energy curve (E_2 and E_3 in Figure 2). Energy level E_2 corresponds to an unbounded motion, and energy level E_3 corresponds to a bound motion.

For the case of non-radial motion, it is convenient to orient the spatial part of the Schwarzschild system of coordinates in such a way that the trajectory of the particle lies in the plane $\theta = 0$. Then, it is necessary to solve both equations for $\tilde{a}_{lm}$ (22) and for $\tilde{b}_{lm}$ (26). The electromagnetic spectrum can be calculated using (36). The simplest case of bound motion is a circular orbit. The calculation of radiation in this case was performed in [62].

The mechanical energy level E_2 corresponds to unbound orbits. An example for calculations of the multipole moments for this case is presented in Figure 5. It can be seen from the figure that, in the case of non-bound orbits, there is a qualitative difference with the case of radially falling charge: the spectrum in the former case has two local maxima.

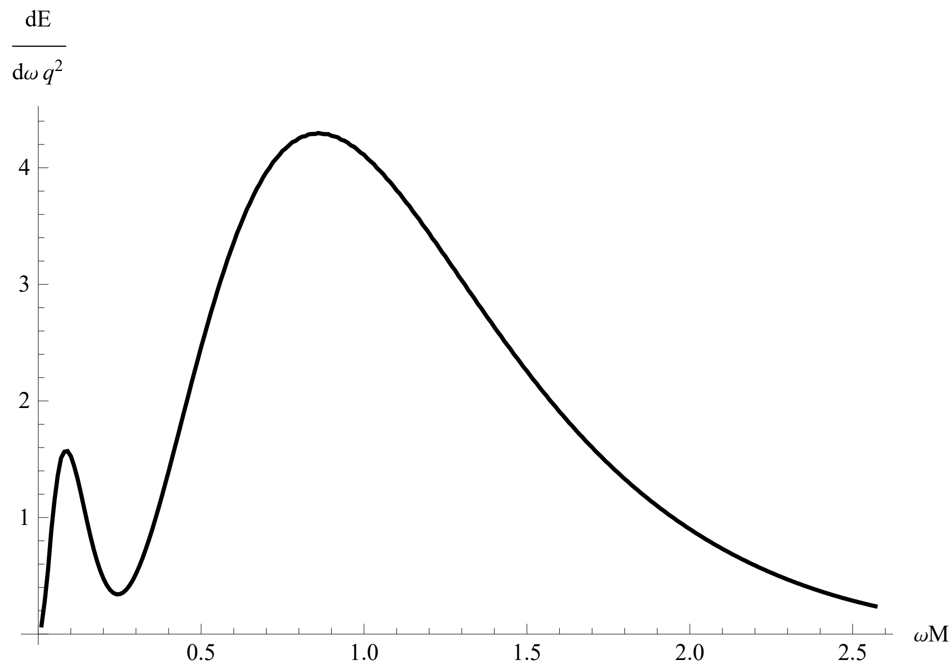

Figure 5. The energy spectrum (for multipole $l = 1, m = 0$), radiated by the particle, moving along the unbound orbit (see Figure 3) in the Schwarzschild geometry.

9. Stationary Component of Electromagnetic Field

Consider test particles moving in the vicinity of a Schwarzschild black hole. This system as a whole will have some non-zero charge of non-zero electric multipole moments, which create the electric field. For the determination of this field, it is sufficient to consider the field created by only one test charge. Then, the field cheated by the system of test charges can be found using the superposition principle.

Solutions for the electric field of one test charge and circular charged ring that are fixed in space are considered, e.g., in [15,66], respectively. In a more realistic situation, the motion of the particle in an external gravitational field should be taken into account. This problem was recently addressed in [41].

Consider the electromagnetic field of the particle radially falling into a black hole. The monopole component of this field can be obtained using Stokes theorem. From Maxwell's Equation (2),

$$q = \int_{\Sigma} j^i \mathrm{d}S_i = \frac{1}{4\pi} \int_{\Sigma} F^{ij}{}_{;j} \mathrm{d}S_i = \frac{1}{4\pi} \oint_{\sigma} F^{ij} \mathrm{d}\sigma_{ij} \,, \tag{53}$$

where Σ is a spacelike hypersurface, which can be chosen as $t = \text{const}$, and σ is a closed surface in S, which can be chosen as sphere $t = \text{const}$, $r = \text{const}$. Then,

$$b_0(r,t) = r^2(F^{10})_0 = \begin{cases} -q\,, \text{ when the charge is inside the surface } \sigma\,, \\ 0\,, \text{ when the charge is outside the surface } \sigma\,. \end{cases} \tag{54}$$

Here, $(F^{10})_0$ denotes the monopole term in multipole expansion of F^{10}.

Other multipole components of the electromagnetic field $b_l(r^*,\omega)$ can be determined from equation (48). For this purpose, we note that this equation mathematically coincides with the Schrodinger equation in quantum mechanics for the particle in potential $U(r^*)$. The approximate solution of this equation can be found using the following approximation, see [41]

$$U(r^*) \approx U_0\delta(r^* - r_0^*)\,, \tag{55}$$

where U_0 is a constant (see Figure 6). Choose two linearly independent solutions of (48) in the following form:

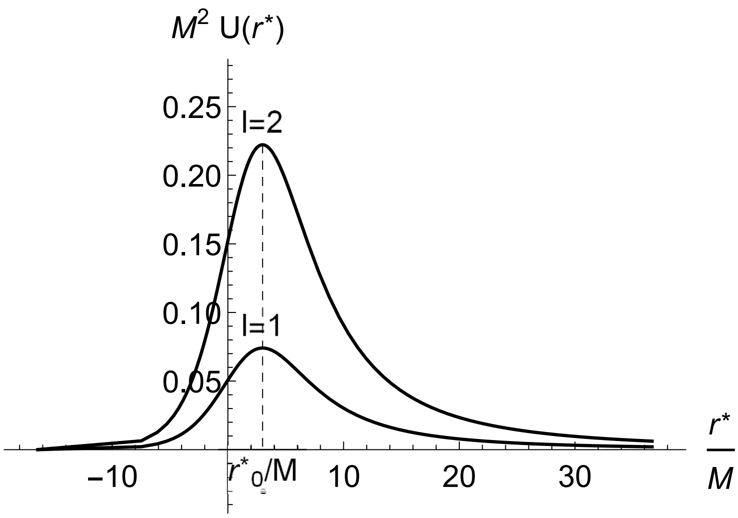

Figure 6. Potential barrier of the Regge–Wheeler equation for multipole moments $l = 1$ and $l = 2$.

$$y_1(r^*) = \begin{cases} e^{-i\omega r^*}\,, & r < 3M\,, \\ Ce^{-i\omega r^*} + De^{i\omega r^*}\,; & r > 3M\,; \end{cases} \tag{56}$$

and

$$y_2(r^*) = \begin{cases} Ce^{i\omega r^*} + De^{-i\omega r^*}\,, & r < 3M\,; \\ e^{i\omega r^*}\,, & r > 3M\,, \end{cases} \tag{57}$$

where coefficients are (see, e.g., [66])

$$C = 1 - \tfrac{U_0}{2i\omega}\,; \tag{58}$$

$$D = \tfrac{D}{2i\omega}e^{-2i\omega\cdot 3M^*}\,; \tag{59}$$

$$W = 2i\omega C = 2i\omega - U_0\,. \tag{60}$$

Due to the asymptotic form of (56) and (57) for $r^* \to \pm\infty$, it follows from (26) that boundary conditions (30b) and (30a) are satisfied for the functions $y_1(r^*)$ and $y_2(r^*)$, respectively. Term I in (51a) has the following form:

$$\begin{aligned} &\frac{q}{2\pi}\frac{2l+1}{l(l+1)}\frac{U_0}{i\omega}\frac{e^{i\omega r^*}}{2i\omega-U_0}\int\limits_{-\infty}^{r^*}\delta(x-r_0^*)e^{-ix\omega}e^{i\omega T(x)}\mathrm{d}x \\ &=\frac{q}{2\pi}\frac{2l+1}{l(l+1)}\frac{U_0}{i\omega}\frac{e^{i\omega(r^*+T(r_0^*)-r_0^*)}}{2i\omega-U_0}\,. \end{aligned} \tag{61}$$

The inverse Fourier transform gives

$$U_0\frac{q}{2\pi}\frac{2l+1}{l(l+1)}\int\limits_{-\infty}^{+\infty}\frac{e^{i\omega(r^*+T(r_0^*)-r_0^*-t)}}{i\omega(2i\omega-U_0)}\mathrm{d}\omega\,. \tag{62}$$

The integral (62) can be carried out using Cauchy's residue theorem. The contour of integration depends on the sign of the factor under the exponent. Due to this, consider two cases. For $r^*+T(r_0^*)-r_0^*-t>0$, one has

$$\begin{aligned} b_l &= \pi i\,\underset{\omega=0}{res}\left[U_0\frac{q}{2\pi}\frac{2l+1}{l(l+1)}\frac{e^{i\omega(r^*+T(r_0^*)-r_0^*-t)}}{i\omega(2i\omega-U_0)}\right] \\ &= -\frac{\rho}{2}\frac{2l+1}{l(l+1)}\,. \end{aligned} \tag{63}$$

If $r^*+T(r_0^*)-r_0^*-t<0$, one has

$$\begin{aligned} b_l &= -\pi i\,\underset{\omega=0}{res}\left[U_0\frac{q}{2\pi}\frac{2l+1}{l(l+1)}\frac{e^{i\omega(r^*+T(r_0^*)-r_0^*-t)}}{i\omega(2i\omega-U_0)}\right] \\ &-2\pi i\underset{\omega=-iU_0/2}{res}\left[U_0\frac{\rho}{2\pi}\frac{2l+1}{l(l+1)}\frac{e^{i\omega(r^*+T(r_0^*)-r_0^*-t)}}{i\omega(2i\omega-U_0)}\right] \\ &= \frac{q}{2}\frac{2l+1}{l(l+1)}-\rho\frac{2l+1}{l(l+1)}e^{\frac{U_0}{2}\omega(r^*+T(r_0^*)-r_0^*-t)}\,. \end{aligned} \tag{64}$$

Substituting (63) and (64) into (51a), we finally obtain

$$b_l(r(r^*),t)=\begin{cases} -\rho\dfrac{2l+1}{l(l+1)}\,, \\ \text{if } T(r^*)<t<r^*+T(r^*)-r_0^*\,; \\ -\rho\dfrac{2l+1}{l(l+1)}e^{\frac{U_0}{2}\omega(r^*+T(r_0^*)-r_0^*-t)}\,, \\ \text{if } t>r^*+T(r_0^*)-r_0^*\,. \end{cases} \tag{65}$$

It follows from (65) that all multipole moments with $l\leq 1$ tend to zero when the test charge approaches the event horizon of the black hole. The same conclusion is obtained with a rectangular potential approximation of $U(r^*)$, see [41].

10. Conclusions

The motion and radiation of charged particles in the vicinity of black holes is a fundamental subject, which is on the basis of virtually all models of relativistic astrophysical objects such as accreting black holes, neutron stars, quasars, etc. Hence, the study of this problem is essential. Given the difficulty of the problem, it was approached with several steps.

We provided a concise review of the most relevant works related to the electromagnetic radiation of a particle in the vicinity of a black hole. Recently, the interest in these works has been revived in the context of models of energy extraction from a black hole.

The first attempts to study electromagnetic fields of a charged particle in the vicinity of a spherically symmetric black hole were based on the assumption that the particle is at rest.

Out of these works, it became clear that when the particle is located on the event horizon, the electric field becomes spherically symmetric. This fact is important for astrophysical models involving charge accretion by a black hole. Indeed, when charges of opposite signs are accreted in equal amounts, the black hole remains uncharged. Instead, when there is a preferential accretion of a charge of a certain sign, the black hole appears to a distant observer to be charged. The same result holds for magnetized black holes.

Analysis of the electromagnetic radiation of a charged particle moving in the vicinity of a spherically symmetric black hole was performed, assuming that the radiation reaction is negligible. Recently, we considered [41] the case of radial infall. Our results, based on the approximate solution of the Regge–Wheeler equation, show that when the particle approaches the event horizon all multipoles, but the monopole, decrease exponentially with time. Hence, the analysis of the dynamical problem leads to the same conclusion as discussed above.

To our knowledge, there is a gap in the literature considering motion and electromagnetic radiation of the particle with arbitrary initial conditions corresponding to different types of motion as presented in Figure 2. We hope to stimulate such general analysis, as it is required for realistic astrophysical models of accreting black holes.

Funding: The work is supported by the BRFFR Foundation in the framework of the F23ICR-003 BRFFR-ICRANet project.

Data Availability Statement: No new data were created or analyzed in this study.

Conflicts of Interest: The authors declare no conflicts of interest.

References

1. Stuchlík, Z.; Kološ, M. Acceleration of the charged particles due to chaotic scattering in the combined black hole gravitational field and asymptotically uniform magnetic field. *Eur. Phys. J. C* **2016**, *76*, 32. [CrossRef]
2. Tursunov, A.; Stuchlík, Z.; Kološ, M.; Dadhich, N.; Ahmedov, B. Supermassive Black Holes as Possible Sources of Ultrahigh-energy Cosmic Rays. *Astrophys. J.* **2020**, *895*, 14. [CrossRef]
3. Kološ, M.; Tursunov, A.; Stuchlík, Z. Radiative Penrose process: Energy gain by a single radiating charged particle in the ergosphere of rotating black hole. *Phys. Rev. D* **2021**, *103*, 024021. [CrossRef]
4. Levin, J.; D'Orazio, D.J.; Garcia-Saenz, S. Black hole pulsar. *Phys. Rev. D* **2018**, *98*, 123002. [CrossRef]
5. Adari, P.; Berens, R.; Levin, J. Charging up boosted black holes. *Phys. Rev. D* **2023**, *107*, 044055. [CrossRef]
6. Karas, V.; Stuchlík, Z. Magnetized Black Holes: Interplay between Charge and Rotation. *Universe* **2023**, *9*, 267. [CrossRef]
7. King, A.R.; Pringle, J.E. Can the Blandford-Znajek Mechanism Power Steady Jets? *Astrophys. J.* **2021**, *918*, L22. [CrossRef]
8. Komissarov, S.S. Electrically charged black holes and the Blandford-Znajek mechanism. *Mon. Not. Roy. Astr. Soc.* **2022**, *512*, 2798–2805. [CrossRef]
9. Ruffini, R.; Rueda, J.A.; Moradi, R.; Wang, Y.; Xue, S.S.; Becerra, L.; Bianco, C.L.; Chen, Y.C.; Cherubini, C.; Filippi, S.; et al. The inner engine of GeV-radiation-emitting gamma-ray bursts. *arXiv* **2019**, arXiv:1811.01839.
10. Ruffini, R.; Moradi, R.; Rueda, J.A.; Becerra, L.; Bianco, C.L.; Cherubini, C.; Filippi, S.; Chen, Y.C.; Karlica, M.; Sahakyan, N.; et al. On the GeV Emission of the Type I BdHN GRB 130427A. *Astrophys. J.* **2019**, *886*, 82. [CrossRef]
11. Ruffini, R.; Rueda, J.A. The blackholic quantum. *Eur. Phys. J. C* **2020**, *80*, 300.
12. Rueda, J.A.; Ruffini, R.; Kerr, R.P. Gravitomagnetic Interaction of a Kerr Black Hole with a Magnetic Field as the Source of the Jetted GeV Radiation of Gamma-Ray Bursts. *Astrophys. J.* **2022**, *929*, 56. [CrossRef]
13. Galt'sov, D.V. *Particles and Fields in the Vicinity of Black Holes*; Moscow University Press: Moscow, Russia, 1986.
14. Copson, E. On Electrostatics in a Gravitational Field. *Proc. R. Soc.* **1928**, *A 118*, 184–194. [CrossRef]
15. Linet, B. Electrostatics and magnetostatics in the Schwarzschild metric. *J. Phys. A Math. Gen.* **1976**, *9*, 1081–1087. [CrossRef]
16. Hanni, R.; Ruffini, R. Lines of Force of a Point Charge near a Schwarzschild Black ole. *Phys. Rev. D* **1973**, *8*, 3259–3265. [CrossRef]
17. Petterson, J.A. Magnetic field of a current loop around a Schwarzschild black hole. *Phys. Rev. D* **1974**, *10*, 3166–3170. [CrossRef]
18. Bicak, J.; Dvorak, L. Stationary electromagnetic fields around black holes i. general solutions and the fields of some special sources near a schwarzschild black hole. *Czech. J. Phys. B* **1977**, *27*, 127–147.
19. Kofron, D.; Kotlarik, P. Debye superpotential for charged rings or circular currents around Kerr black hole. *Phys. Rev. D* **2022**, *106*, 104022. [CrossRef]

20. Ross, D.K. Radiation from particles falling into black-holes. *Pab. Astron. Soc. Pac.* **1971**, *83*, 633–637. [CrossRef]
21. Breuer, R.A.; Ruffini, R.; Tiomno, J.; Vishveshwara, C.V. Vector and Tensor Radiation from Schwarzschild Relativistic Circular Geodesics. *Phys. Rev. D* **1973**, *7*, 1002–1007. [CrossRef]
22. Breuer, R.A.; Chrzanowksi, P.L.; Hughes, H.G.; Misner, C.W. Geodesic Synchrotron Radiation. *Phys. Rev. D* **1973**, *8*, 4309–4319. [CrossRef]
23. Aliev, A.N.; Gal'tsov, D.V. Reviews of Topical Problems: "Magnetized" black holes. *Sov. Phys. Uspekhi* **1989**, *32*, 75–92. [CrossRef]
24. Pugliese, D.; Quevedo, H.; Ruffini, R. Motion of charged test particles in Reissner-Nordström spacetime. *Phys. Rev. D* **2011**, *83*, 104052. [CrossRef]
25. Dymnikova, I.G. High-Frequency Radiation from a Particle Falling into a Kerr Black Hole. *Astrophys. Space Sci.* **1977**, *51*, 229–234. [CrossRef]
26. Dymnikova, I.G.; Popov, A.K. Low-Frequency Radiation from a Particle Falling Into a Kerr Black Hole. *Astrophys. Space Sci.* **1980**, *68*, 487–494. [CrossRef]
27. Prasanna, A.R. General-relativistic analysis of charged-particle motion in electromagnetic fields surrounding black holes. *Nuovo C. Riv. Ser.* **1980**, *11*, 1–53. [CrossRef]
28. Abdujabbarov, A.A.; Ahmedov, B.J.; Jurayeva, N.B. Charged-particle motion around a rotating non-Kerr black hole immersed in a uniform magnetic field. *Phys. Rev. D* **2013**, *87*, 064042. [CrossRef]
29. Frolov, V.P.; Shoom, A.A. Motion of charged particles near a weakly magnetized Schwarzschild black hole. *Phys. Rev. D* **2010**, *82*, 084034. [CrossRef]
30. Shiose, R.; Kimura, M.; Chiba, T. Motion of charged particles around a weakly magnetized rotating black hole. *Phys. Rev. D* **2014**, *90*, 124016. [CrossRef]
31. Kološ, M.; Stuchlík, Z.; Tursunov, A. Quasi-harmonic oscillatory motion of charged particles around a Schwarzschild black hole immersed in a uniform magnetic field. *Class. Quantum Gravity* **2015**, *32*, 165009. [CrossRef]
32. Tursunov, A.; Stuchlík, Z.; Kološ, M. Circular orbits and related quasiharmonic oscillatory motion of charged particles around weakly magnetized rotating black holes. *Phys. Rev. D* **2016**, *93*, 084012. [CrossRef]
33. Al Zahrani, A.M. Charged Particle Circular Orbits around Weakly Charged and Magnetized Kerr Black Holes. *Astrophys. J.* **2022**, *937*, 50. [CrossRef]
34. Ruffini, R.; Tiomno, J.; Vishveshwara, C.V. Electromagnetic field of a particle moving in a spherically symmetric black-hole background. *Nuovo C. Lett.* **1972**, *3*, 211–215. [CrossRef]
35. Tiomno, J. Maxwell Equations in a Spherically Symmetric Black-Hole Background and Radiation by a Radially Moving Charge. *Lett. Nuovo C.* **1972**, *5*, 851–855. [CrossRef]
36. Ruffini, R. Fully relativistic treatment of the breahmstrahlung radiation from a charge falling in a strong gravitational field. *Phys. Let.* **1972**, *41B*, 334–338. [CrossRef]
37. Folacci, A.; Ould El Hadj, M. Electromagnetic radiation generated by a charged particle falling radially into a Schwarzschild black hole: A complex angular momentum description. *Phys. Rev. D* **2020**, *102*, 024026. [CrossRef]
38. Regge, T.; Wheeler, J.A. Stability of a Schwarzschild Singularity. *Phys. Rev.* **1957**, *108*, 1063–1069. [CrossRef]
39. Zerilli, F.J. Gravitational Field of a Particle Falling in a Schwarzschild Geometry Analyzed in Tensor Harmonics. *Phys. Rev. D* **1970**, *2*, 2141–2160. [CrossRef]
40. Teukolsky, S.A. Perturbations of a Rotating Black Hole. I. Fundamental Equations for Gravitational, Electromagnetic, and Neutrino-Field Perturbations. *Astrophys. J.* **1973**, *185*, 635–648. [CrossRef]
41. Komarov, S.O.; Gorbatsievich, A.K.; Vereshchagin, G.V. Electromagnetic field of a charge asymptotically approaching a spherically symmetric black hole. *Phys. Rev. D* **2023**, *108*, 104056. [CrossRef]
42. Shatskiya, A.A.; Novikova, I.D.; Lipatovaa, L.N. Spectrum of Relativistic Radiation from Electric Charges and Dipoles as They Fall Freely into a Black Hole. *J. Exp. Theor. Phys.* **2013**, *116*, 904–910. [CrossRef]
43. Fiziev, P.P. Exact solutions of Regge–Wheeler equation and quasi-normal modes of compact objects. *Class. Quantum Grav.* **2006**, *23*, S175–S178. [CrossRef]
44. Leaver, E.W. Spectral decomposition of the perturbation response of the Schwarzschild geometry. *Phys. Rev. D* **1986**, *34*, 384–408. [CrossRef] [PubMed]
45. Folacci, A.; Ould El Hadj, M. Alternative description of gravitational radiation from black holes based on the Regge poles of the S-matrix and the associated residues. *Phys. Rev. D* **2018**, *98*, 064052. [CrossRef]
46. Chandrasekhar, S.; Ferrari, V. On the non-radial oscillations of a star. IV—An application of the theory of Regge poles. *Proc. R. Soc. Lond. Ser. A* **1992**, *437*, 133–149. [CrossRef]
47. Folacci, A.; Ould El Hadj, M. Electromagnetic radiation generated by a charged particle plunging into a Schwarzschild black hole: Multipolar waveforms and ringdowns. *Phys. Rev. D* **2018**, *98*, 024021. [CrossRef]
48. Shoom, A. Synchrotron radiation from a weakly magnetized Schwarzschild black hole. *Phys. Rev. D* **2015**, *92*, 124066. [CrossRef]

49. Tursunov, A.; Kološ, M.; Stuchlík, Z.; Gal'tsov, D.V. Radiation Reaction of Charged Particles Orbiting a Magnetized Schwarzschild Black Hole. *Astrophys. J.* **2018**, *861*, 16. [CrossRef]
50. Misner, C.W.; Thorne, K.S.; Wheeler, J.A. *Gravitation*; W. H. Freeman and Company: San Francisco, CA, USA, 1973.
51. Poisson, E.; Pound, A.; Vega, I. The Motion of Point Particles in Curved Spacetime. *Living Rev. Relativ.* **2011**, *14*, 190. [CrossRef] [PubMed]
52. Sing, J. *Relativity: The General Theory*; North-Holland Publishing Company: Amsterdam, The Netherlands, 1960.
53. Stephani, H. *Relativity. An introduction to Special and General Relativity*, 3rd ed.; Cambridge University Press: Cambridge, UK, 2004.
54. Santos, J.S.; Cardoso, V.; Natario, J. Electromagnetic radiation reaction and energy extraction from black holes: The tail term cannot be ignored. *Phys. Rev. D* **2003**, *107*, 064046. [CrossRef]
55. Dewitt, C.M.; Dewitt, B. Falling charges. *Physics* **1964**, *1*, 3–20. [CrossRef]
56. Pfenning, M.J.; Poisson, E. Scalar, electromagnetic, and gravitational self-forces in weakly curved spacetimes. *Phys. Rev. D* **2002**, *65*, 084001. [CrossRef]
57. Komarov, S.O.; Gorbatsievich, A.K.; Garkun, A.S.; Vereshchagin, G.V. Electromagnetic Radiation and Electromagnetic Self-Force of a Point Charge in the Vicinity of the Schwarzschild Black Hole. *Nonlinear Phenom. Complex Syst.* **2023**, *26*, 77–82.
58. Thorne, K.S.; Price, R.H.; Macdonald, D.A. *Black Holes: The Membrane Paradigm;* Yale University Press: New Haven, CT, USA; London, UK, 1986; pp. 49–52.
59. McGruder, C.H. Field Energies and principles of equivalence. *Nature* **1978**, *272*, 806–807. [CrossRef]
60. Vilenkin, A. Self-interaction of charged particles in the gravitational field. *Phys. Rev. D* **1979**, *2*, 373–376. [CrossRef]
61. Smith, A.G.; Will, C.M. Force on a static charge outside a Schwarzschild black hole. *Phys. Rev. D* **1980**, *22*, 1276–1284. [CrossRef]
62. Ruffini, R. On the energetics of black holes. In *Black Holes (Les Astres Occlus)*; Gordon and Breach: New York, NY, USA 1973; pp. 451–546.
63. Korn, G.A.; Korn, T.M. *Mathematical Handbook for Scientists and Engineers; Definitions, Theorems and Formulas for Reference and Review*; McGraw-Hill Book Company: New York, NY, USA, 1968.
64. Thorne, K.S.; Price, R.H.; Macdonald, D.A. *Black Holes: The Membrane Paradigm*; Yale University Press: New Haven, CT, USA; London, UK, 1986; pp. 23–25.
65. Cardoso, V.; Lemos, J.P.; Yoshida, S. Electromagnetic radiation from collisions at almost the speed of light: An extremely relativistic charged particle falling into a Schwarzschild black hole. *Phys. Rev. D* **2003**, *68*, 084011. [CrossRef]
66. Flugge, S. *Practical Quantum Mechanics*; Springer: Berlin/Heidelberg, Germany, 1994; 287p.